JCI The Journal of Clinical Investigation

CotH3 mediates fungal invasion of host cells during mucormycosis

Teclegiorgis Gebremariam, … , Michael R. Yeaman, Ashraf S. Ibrahim

J Clin Invest. 2014;124(1):237-250. https://doi.org/10.1172/JCI71349.

Research Article

Angioinvasion is a hallmark of mucormycosis. Previously, we identified endothelial cell glucose-regulated protein 78 (GRP78) as a receptor for Mucorales that mediates host cell invasion. Here we determined that spore coat protein homologs (CotH) of Mucorales act as fungal ligands for GRP78. CotH proteins were widely present in Mucorales and absent from noninvasive pathogens. Heterologous expression of *CotH3* and *CotH2* in *Saccharomyces cerevisiae* conferred the ability to invade host cells via binding to GRP78. Homology modeling and computational docking studies indicated structurally compatible interactions between GRP78 and both CotH3 and CotH2. A mutant of *Rhizopus oryzae*, the most common cause of mucormycosis, with reduced CotH expression was impaired for invading and damaging endothelial cells and CHO cells overexpressing GRP78. This strain also exhibited reduced virulence in a diabetic ketoacidotic (DKA) mouse model of mucormycosis. Treatment with anti-CotH Abs abolished the ability of *R. oryzae* to invade host cells and protected DKA mice from mucormycosis. The presence of CotH in Mucorales explained the specific susceptibility of DKA patients, who have increased GRP78 levels, to mucormycosis. Together, these data indicate that CotH3 and CotH2 function as invasins that interact with host cell GRP78 to mediate pathogenic host-cell interactions and identify CotH as a promising therapeutic target for mucormycosis.

CotH3 mediates fungal invasion of host cells during mucormycosis

Teclegiorgis Gebremariam,[1,2] Mingfu Liu,[1,2] Guanpingsheng Luo,[1,2] Vincent Bruno,[3] Quynh T. Phan,[1,2] Alan J. Waring,[4,5] John E. Edwards Jr.,[1,2,5] Scott G. Filler,[1,2,5] Michael R. Yeaman,[1,2,4,5] and Ashraf S. Ibrahim[1,2,5]

[1]Division of Infectious Diseases, Harbor-UCLA Medical Center, Torrance, California, USA. [2]St. John's Cardiovascular Research Center, Los Angeles Biomedical Research Institute at Harbor-UCLA Medical Center, Torrance, California, USA. [3]Institute for Genome Sciences, Department of Microbiology and Immunology, University of Maryland School of Medicine, Baltimore, Maryland, USA. [4]Division of Molecular Medicine, Harbor-UCLA Medical Center, Torrance, California, USA. [5]David Geffen School of Medicine at UCLA, Los Angeles, California, USA.

Angioinvasion is a hallmark of mucormycosis. Previously, we identified endothelial cell glucose-regulated protein 78 (GRP78) as a receptor for Mucorales that mediates host cell invasion. Here we determined that spore coat protein homologs (CotH) of Mucorales act as fungal ligands for GRP78. CotH proteins were widely present in Mucorales and absent from noninvasive pathogens. Heterologous expression of *CotH3* and *CotH2* in *Saccharomyces cerevisiae* conferred the ability to invade host cells via binding to GRP78. Homology modeling and computational docking studies indicated structurally compatible interactions between GRP78 and both CotH3 and CotH2. A mutant of *Rhizopus oryzae*, the most common cause of mucormycosis, with reduced CotH expression was impaired for invading and damaging endothelial cells and CHO cells overexpressing GRP78. This strain also exhibited reduced virulence in a diabetic ketoacidotic (DKA) mouse model of mucormycosis. Treatment with anti-CotH Abs abolished the ability of *R. oryzae* to invade host cells and protected DKA mice from mucormycosis. The presence of CotH in Mucorales explained the specific susceptibility of DKA patients, who have increased GRP78 levels, to mucormycosis. Together, these data indicate that CotH3 and CotH2 function as invasins that interact with host cell GRP78 to mediate pathogenic host-cell interactions and identify CotH as a promising therapeutic target for mucormycosis.

Introduction

Mucormycosis is a life-threatening infection with very poor outcome despite current treatment options, which include surgical debridement of infected foci and antifungal therapy (1–3). Mortality rates for mucormycosis often exceed 40% and can approach 100% in patients with disseminated disease, persistent neutropenia, or cerebral invasion (4, 5). Even patients who survive the infection are typically left with considerable disfigurement from surgical interventions (1, 6). Therefore, new intervention and/or treatment therapies are urgently needed.

The disease is caused by various fungi belonging to the order Mucorales, among which *Rhizopus oryzae* is the most common. This organism is responsible for up to 70% of all cases of mucormycosis (3, 7, 8). Although patients with a weakened immune system (e.g., due to hematologic malignancy, organ transplantation, or trauma such as the Joplin tornado or the Indian Ocean tsunami; refs. 1, 9, 10), prematurity, or malnourishment (1, 11) are at increased risk of mucormycosis, hyperglycemia, diabetic ketoacidosis (DKA), and other forms of acidosis uniquely predispose patients to mucormycosis (1, 4, 12).

Despite the differing predisposing factors, mucormycosis is characterized by the propensity of all Mucorales to invade the vasculature, resulting in blood vessel thrombosis and subsequent tissue necrosis (1, 4, 13). Thus, fungal interaction with endothelial cells lining the vasculature represents an important step in the pathogenesis of mucormycosis. Previously, we determined that *R. oryzae* strains adhere to human umbilical vein endothelial cells in vitro and invade these cells by induced endocytosis (14). We recently discovered glucose-regulated protein 78 (GRP78) as the endothelial cell receptor to which Mucorales bind during host cell invasion (15). Elevated concentrations of glucose and iron, consistent with those seen during hyperglycemia, DKA, or other forms of acidosis, enhance GRP78 expression, leading to fungal invasion and damage of endothelial cells in a receptor-dependent manner (15). Finally, DKA mice, which express more GRP78 in the target organs than normal mice, are protected from mucormycosis when given anti-GRP78 Abs (15). Collectively, these results explain, at least in part, the unique mucormycosis susceptibility of hyperglycemic and DKA patients, as well as those with other forms of acidosis. In the current study, we sought to identify the fungal cell surface protein that binds to GRP78 and its role in the pathogenesis of mucormycosis. We provide evidence that the spore coat protein homolog (CotH) cell surface proteins, in particular CotH3, are the fungal ligands that mediate attachment to GRP78 during host cell invasion. Importantly, Abs against CotH protected mice from mucormycosis, which suggests that CotH is a promising target for passive or active immunotherapy. Of equal importance was the wide presence of CotH proteins among Mucorales and their absence from other pathogens, further explaining the hypersusceptibility of hosts that overexpress GRP78.

Results

Isolation of putative R. oryzae ligands that bind endothelial cell GRP78. Far-Western blot analysis (16) using recombinant human GRP78 and anti-GRP78 Abs revealed the presence of 4 bands collected from the supernatant of *R. oryzae* protoplasts that bound to GRP78 (Figure 1A). These bands were excised for protein identification

Conflict of interest: The authors have declared that no conflict of interest exists.
Citation for this article: *J Clin Invest.* 2014;124(1):237–250. doi:10.1172/JCI71349.

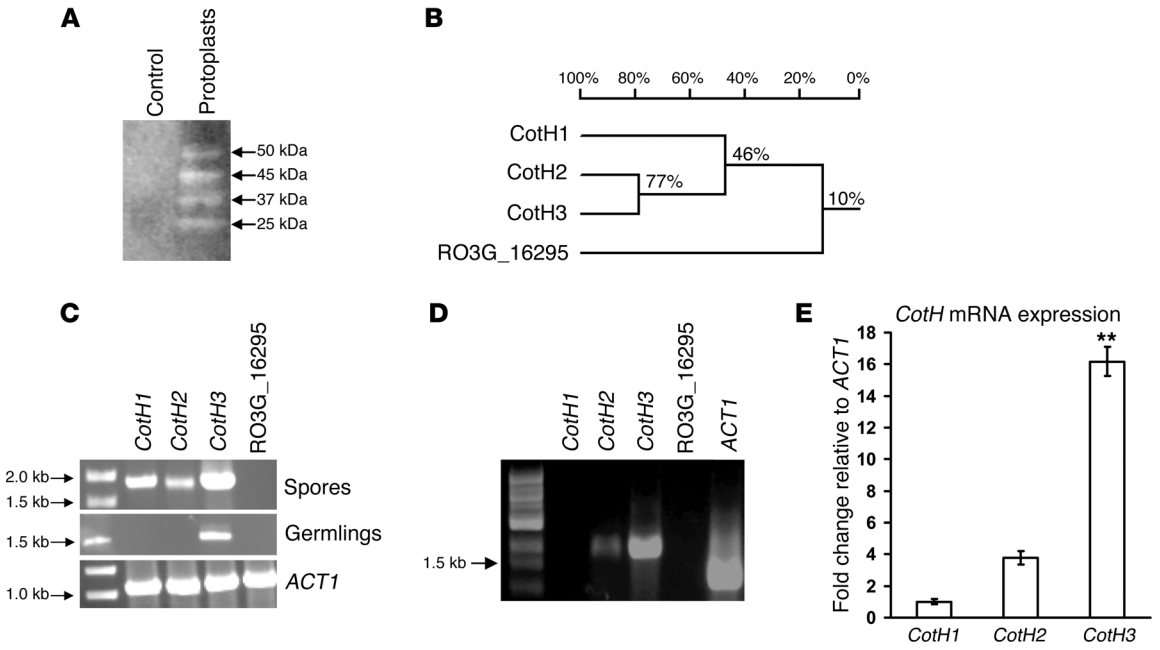

Figure 1

Identification and expression of *CotH* genes. (**A**) Far-Western blot of *R. oryzae* surface proteins that bound to GRP78. (**B**) Dendrogram showing the close identity between CotH2 and CotH3 predicated proteins and the divergence of the CotH proteins from RO3G_16295, the fourth identified ORF widely present in fungi without an identified function. (**C**) All 3 *CotH* genes were expressed in resting spores, but only *CotH3* was expressed in germlings, of *R. oryzae* grown in YPD at 37°C. *ACT1* represents the loading control. Lanes were run on the same gel but were noncontiguous. (**D**) Exposure of *R. oryzae* germlings to endothelial cells induced expression of only *CotH2* and *CotH3*, as determined by RT-PCR. (**E**) Quantification of *CotH* mRNA expression in *R. oryzae* germlings on endothelial cells by qRT-PCR (relative to *ACT1*) demonstrated 16- and 4-fold increases in *CotH3* and *CotH2* expression, respectively, whereas *CotH1* had no detectable expression. RO3G_16295 was not expressed under any condition tested. $^{**}P < 0.001$ vs. *CotH1* and *CotH2*, Wilcoxon rank-sum test. $n = 9$ from 3 independent experiments.

by MALDI-TOF–mass spectrometry/mass spectrometry analysis. Only 4 ORFs predicted to be cell surface proteins were identified with GPI anchor sequence at the C terminus, signal peptides at the N terminus, and multiple predicted N- and O-glycosylation sites. 3 of the ORFs — RO3G_05018, RO3G_08029, and RO3G_11882 — had limited homology (17% at the amino acid level) to the CotH family of proteins, which have been implicated in spore coat formation from several bacteria (17, 18). These were named *CotH1* (RO3G_05018), *CotH2* (RO3G_08029) and *CotH3* (RO3G_11882). The fourth ORF, RO3G_16295, was widely present in many fungi and some bacteria without an identified function.

The predicted CotH2 and CotH3 were closely related, with 77% identity at the amino acid level, while CotH1 was more distantly related (Figure 1B). The fourth ORF had an overall identity of 10% to the 3 CotH proteins. Upon searching the *R. oryzae* 99-880 (also known as *R. delemar*) genome database, we found 2 more related ORFs predicted to encode GPI-anchored proteins. These were named *CotH4* (RO3G_09276) and *CotH5* (RO3G_01139), but were not further pursued, because their products were unlikely to interact with GRP78 (they did not show in our far-Western blot analysis) and because of their distant homology to original CotH1, CotH2, and CotH3 (20%–24% at the amino acid level).

We also examined whether this family of genes was present in other Mucorales known to cause human mucormycosis. Using primers that spanned the entire *CotH3* ORF (1.9 kb), we were able to amplify bands from clinical isolates of *R. oryzae* 99-892, *Mucor* sp. 99-932, *Lichtheimia corymbifera*, *Cunninghamella bertholletiae*, and *Rhizomucor* spp. Subsequent data generated from genome sequencing projects initiated by the Broad Institute, University of Jena, University of Maryland, and Los Angeles Biomedical Research Institute confirmed our findings that orthologs of *CotH1*–*CotH3* were present in every Mucorales genome analyzed, with percent identity at the amino acid level ranging from 49% (*Mortierella verticillata* CotH1 ortholog) to 82% (*Rhizomucor* CotH2) (Table 1). Furthermore, partial sequence assembly of 5 other Mucorales strongly indicated the presence of this family of genes in these fungi (Table 1). Collectively, these studies demonstrated that the *CotH* gene family is commonly present in Mucorales family members.

CotH2 and CotH3 are expressed during interaction of R. oryzae with endothelial cells. We reasoned that if any of the isolated proteins is a true fungal ligand for GRP78, its gene must be expressed during *R. oryzae* interaction with endothelial cells. Because *R. oryzae* germlings bind endothelial cell GRP78 (15), we studied the expression of the *CotH* genes in spores and germlings. When the organism was grown in YPD broth, *CotH1*–*CotH3* were expressed by spores; however, only *CotH3* was expressed by germlings of *R. oryzae* (Figure 1C). Importantly, when *R. oryzae* germlings were incubated on endothelial cells, only *CotH2* and *CotH3* were expressed, with *CotH3* showing the highest level of expression (increased 16- and 4-fold compared with *CotH1* and *CotH2*, respectively; Figure 1, D and E). Finally, expression of the fourth ORF, RO3G_16295, was below the limit of detection in *R. oryzae* spores or germlings in YPD or in *R. oryzae* germlings interacting with endothelial cells (Figure 1, C and D). These results suggest that *CotH3* and, to a lesser extent,

Table 1
Sequence homology of *CotH* genes from *R. oryzae* 99-880 to possible Mucorales orthologs

Strain ID	Mucorales	Source	*CotH1*		*CotH2*		*CotH3*	
			Identity	Positive	Identity	Positive	Identity	Positive
Full sequence								
—	*Lichtheimia corymbifera*	Jena University	54%	71%	55%	72%	59%	70%
—	*Lentamyces parricida*	Jena University	54%	68%	55%	70%	55%	71%
1006 PhL	*Mucor circinelloides*	Broad Institute	69%	79%	67%	79%	73%	83%
NRRL 6337	*Mortierella verticillata*	Broad Institute	49%	62%	57%	71%	57%	72%
—	*Rhizomucor*	Harbor-UCLA Medical Center	NF	NF	82%	89%	79%	87%
Partial sequence								
97-1192	*Mucor racemosus*	University of Maryland	92% (418)	93%	96% (404)	97%	97% (403)	98%
B8987	*Mucor circinelloides*	University of Maryland	70% (339)	80%	67% (401)	80%	71% (399)	80%
B5328	*Mucor velutinous*	University of Maryland	68% (329)	78%	68% (401)	78%	71% (399)	78%
B7407	*Rhizopus oryzae*	University of Maryland	97% (365)	98%	96% (404)	97%	97% (403)	97%
B9770	*Rhizopus stolonifer*	University of Maryland	78% (470)	87%	84% (404)	90%	87% (398)	92%

Numbers in parentheses denote the length of the amino acid stretch that the blast search picked out. NF, not found.

CotH2 are putative candidates for interacting with GRP78 during invasion of human cells.

S. cerevisiae cells expressing CotH2 or CotH3 bind GRP78 and adhere to and invade endothelial cells and CHO cells overexpressing GRP78. To study whether CotH1, CotH2, and CotH3 interact with GRP78, we heterologously expressed the genes for each of these proteins in the nonadherent/noninvasive *S. cerevisiae* and then tested the ability of the transformed yeast cells to bind endothelial cell GRP78. To confirm the cell surface localization of the heterologously expressed genes, we raised Abs against a 16-mer peptide (MGQTNDGAYRDPTDNN) from CotH3, which was predicted to be antigenic and surface exposed and had 78% identity to the corresponding amino acids of CotH1 and CotH2. These Abs recognized *S. cerevisiae* expressing each of the *CotH* genes, but not cells expressing empty plasmid (Supplemental Figure 1; supplemental material available online with this article; doi:10.1172/JCI71349DS1), thereby verifying the cell surface expression of each of the *CotH* genes.

Next, we used the affinity purification process developed by Isberg and Leong (19) to study the ability of *S. cerevisiae* expressing each of the *CotH* genes to interact with endothelial cell GRP78. When incubated with extracts of endothelial cell membrane proteins, *S. cerevisiae* expressing CotH1 or transformed with the empty plasmid (control) did not bind any detectable GRP78 (Figure 2A). In contrast, *S. cerevisiae* cells expressing CotH3 bound more GRP78 than did cells expressing CotH2 (Figure 2A). These results indicate that CotH3 and, to a lesser extent, CotH2 proteins interact with GRP78 in endothelial cell extracts. Next, we examined the ability of the transformed *S. cerevisiae* cells to adhere to and invade endothelial cells in vitro. *S. cerevisiae* containing the empty plasmid or CotH1 protein had minimal adherence to and endocytosis (invasion) by endothelial cells; conversely, *S. cerevisiae* expressing CotH2 or CotH3 proteins had significantly increased adherence to and invasion of endothelial cells compared with the control strain (Figure 2B). Furthermore, cells expressing CotH3 had significantly greater ability to adhere to and invade endothelial cells than did cells expressing CotH2. To examine whether this enhanced adherence to and invasion of endothelial cells was caused by interaction with GRP78, we compared the ability of *S. cerevisiae* expressing CotH1, CotH2, CotH3, or empty plasmid to interact with CHO cells overexpressing hamster GRP78 (20, 21). Only *S. cerevisiae* expressing CotH2 or CotH3 proteins had significant enhancement in adherence to and invasion of GRP78-overexpressing CHO cells, but not parental dihydrofolate reductase–deficient (DHFR-deficient) CHO cells. Again, *S. cerevisiae* cells expressing CotH3 protein demonstrated a greater ability than those expressing CotH2 protein to bind to and invade GRP78-overexpressing CHO cells (Figure 2C). Collectively, these data indicate that CotH3 and, to a lesser extent, CotH2 are potential adhesins/invasins that interact with GRP78.

CotH proteins colocalize with GRP78 during endocytosis of R. oryzae by endothelial cells. If CotH2 and/or CotH3 are the fungal ligands that bind to GRP78, they should interact with GRP78 during *R. oryzae* invasion of endothelial cells. Therefore, we used indirect immunofluorescence to verify that CotH proteins on *R. oryzae* interacted with GRP78 on intact endothelial cells during invasion. As we and others demonstrated previously (15, 22, 23), endothelial cells expressed GRP78 on their surface (Figure 3). When endothelial cells were infected with *R. oryzae* germlings, GRP78 colocalized with *R. oryzae* CotH (Figure 3, A and C). These findings suggest that during *R. oryzae* invasion, CotH proteins interact with GRP78 on intact endothelial cells.

CotH3 is a R. oryzae invasin. Because we previously showed that endocytosis of the fungus is a prerequisite for *R. oryzae* to cause endothelial cell damage (14, 15), we sought to determine whether blocking the function or expression of CotH3 would protect endothelial cells from *R. oryzae*–induced endocytosis and subsequent damage. Endothelial cell endocytosis of *R. oryzae* germlings was abrogated by addition of rabbit anti-CotH3 polyclonal Abs, but not preimmune serum collected from the same animal (Figure 4A). Furthermore, the anti-CotH3 Abs reduced *R. oryzae*–induced damage to endothelial cells by >40% (Figure 4B). Interestingly, the anti-CotH3 Abs had no effect on *R. oryzae* adherence to endothelial cells (Figure 4A). Notably, anti-CotH3 Abs had no effect on *R. oryzae* respiration, germling formation, or growth (Supplemental Figure 2).

To complement the Ab blocking studies, we sought to suppress *CotH3* and *CotH2* mRNA expression in order to determine their effect on adherence, endocytosis, and endothelial cell damage. We used our previously developed RNAi method (24) to suppress both genes simultaneously in 2 independent transformants (Trans 2 and Trans 6) and verified the attenuated expression of CotH pro-

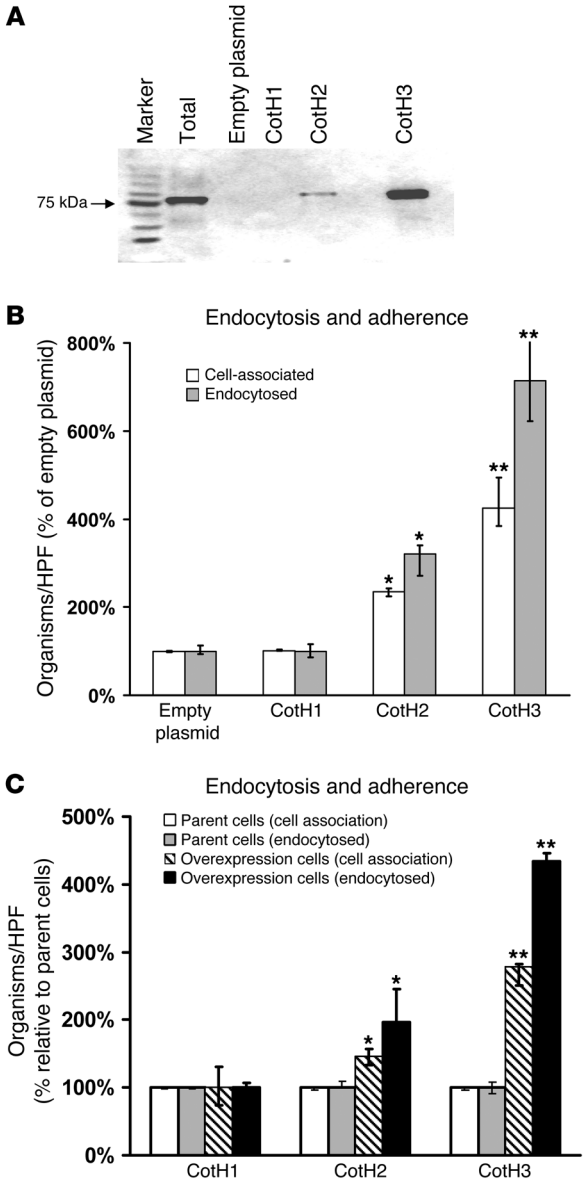

Figure 2

S. cerevisiae cells heterologously expressing CotH2 or CotH3, but not CotH1, interact with host cells through GRP78. (**A**) Endothelial cell surface proteins were labeled with NHS-biotin, then extracted with *n*-octyl-β-D-glucopyranoside in PBS-CM and protease inhibitors. Labeled proteins (250 mg) were incubated with 2×10^8 *S. cerevisiae* cells, after which unbound proteins were removed by extensive rinsing with PBS-CM. The membrane proteins that remained bound to the organisms were eluted with 6 M urea, separated on 10% SDS-PAGE, and identified by immunoblotting with anti-GRP78 Ab. (**B** and **C**) Adherence and endocytosis (determined by differential fluorescence) assays were carried out using endothelial cells (**B**) or GRP78-overexpressing or parent CHO cells (**C**) split on 12-mm glass coverslips. HPF, high-power field. $^*P < 0.001$ vs. empty plasmid or CotH1, $^{**}P < 0.001$ vs. CotH1 and CotH2, Wilcoxon rank-sum test. $n = 9$ from 3 independent experiments. Data are median ± interquartile range.

teins on the fungal cell surface by flow cytometry (Figure 5, A and B). Notably, these RNAi-transformed *R. oryzae* cells had no difference in growth rate, germination, cell size, or respiratory activity compared with wild-type or empty plasmid–transformed *R. oryzae* (Supplemental Figure 3). Importantly, the reduced *R. oryzae* cell surface expression of CotH2 and CotH3 markedly reduced the endothelial cell endocytosis of *R. oryzae* germlings (Figure 3, compare A and B). Additionally, blocking CotH2 and CotH3 expression resulted in diminished CotH staining, and these RNAi-transformed cells did not colocalize with GRP78 (Figure 3D). Concordant with the indirect immunofluorescence experiments, we found that blocking CotH2 and CotH3 expression resulted in an approximately 60% decrease in invasion and subsequent endothelial cell damage (Figure 6, A and B). Collectively, these results indicate that CotH3 and CotH2 are required for maximal invasion of endothelial cells by *R. oryzae*. However, the finding that suppression of CotH expression did not completely block endothelial cell invasion suggests that other invasins may also be involved in *R. oryzae* interaction with endothelial cells.

To confirm that CotH3 and CotH2 function as invasins by interacting with GRP78, we compared wild-type, empty plasmid–transformed, and RNAi-transformed *R. oryzae* germlings for their ability to damage GRP78-overexpressing or parent CHO cells (20, 21). As we previously showed (15), wild-type *R. oryzae* caused considerably more damage to GRP78-overexpressing than to parent CHO cells. As expected, empty plasmid–transformed *R. oryzae* germlings caused a similar amount of damage. In contrast, the RNAi-transformed *R. oryzae* germlings, with reduced cell surface expression of CotH3 and CotH2, caused significantly less damage to the GRP78-overexpressing cells (Figure 6C). Collectively, these results demonstrated that CotH3 and CotH2 are cell surface proteins that mediate invasion (endocytosis) and subsequent damage of endothelial cells via interaction with GRP78.

CotH2 and CotH3 have no effect on cell wall integrity or susceptibility to phagocytes. Because some GPI-anchored proteins are required for cell wall integrity, we sought to determine whether attenuation of CotH2 and CotH3 expression affected cell wall composition and organization. We therefore determined the capacity of wild-type, empty plasmid–transformed, and RNAi-transformed *R. oryzae* to grow in the presence of the cell wall stressors Congo red, calcofluor white, hydrogen peroxide, SDS, and Triton X-100, and found that all strains grew similarly (Supplemental Figure 4). These results indicate that CotH2 and CotH3 proteins are dispensable for cell wall composition and organization. Additionally, empty plasmid– and RNAi-transformed *R. oryzae* were equally susceptible to mouse macrophage- or neutrophil-mediated damage in vitro (Supplemental Figure 5), which indicates that CotH2 and CotH3 are not involved in conferring resistance to phagocyte killing.

Structural basis for CotH protein interactions with GRP78. Consistent with our biological results, computational modeling and in silico docking studies indicated substantial and specific binding of CotH3 and CotH2 to the target GRP78 protein (Figure 7). Interestingly, the homology models of CotH3 and CotH2 were not identical, likely owing to differences in their amino acid sequences (23% nonidentity). Nonetheless, both proteins targeted a similar α-helical bundle domain of GRP78, with the predicted CotH3 contact area being considerably larger and more conformed as a reciprocal GRP78 binding cleft than that of CotH2 (Figure 7). Importantly, peptide MGQTNDGAYRDPTDNN, against which blocking Abs were raised (Figure 4), resided in the

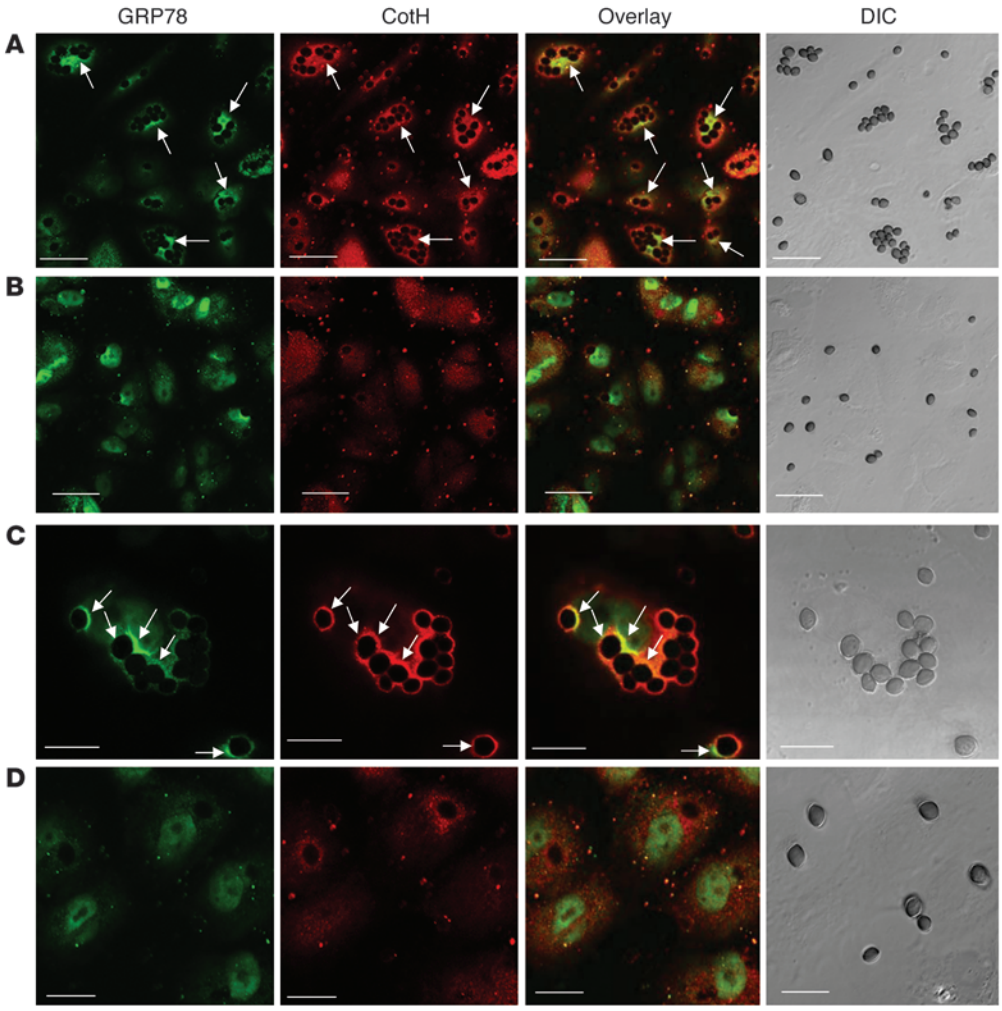

Figure 3
GRP78 on intact endothelial cells colocalizes with *R. oryzae* expressing CotH proteins during endocytosis. Confocal microscopic images of endothelial cells infected with empty plasmid–transformed (**A** and **C**) or *CotH2*/*CotH3* RNAi construct–transformed (**B** and **D**) *R. oryzae* that were germinated for 1 hour. Confluent endothelial cells on a 12-mm-diameter glass coverslip were infected with 10^5 *R. oryzae* germlings. After a 40-minute incubation at 37°C, cells were fixed with 3% paraformaldehyde, washed, blocked, and then stained for GRP78 and CotH. Merged images show colocalization (yellow). The same field was taken with differential interference contrast (DIC) imaging to show the presence of *R. oryzae*. Arrows indicate GRP78 accumulation, CotH cell surface staining, and GRP78/CotH colocalization on *R. oryzae*. Scale bars: 30 μm (**A** and **B**); 15 μm (**C** and **D**).

binding cleft. In contrast, CotH1 exhibited a minimal contact area that targeted a different facet of the GRP78 protein. Collectively, these data supported our biological observations of a hierarchical binding relationship with respect to GRP78 (in descending order: CotH3, CotH2, CotH1).

CotH2 and CotH3 are required for full virulence of R. oryzae in vivo. Because *CotH3* and *CotH2* encode invasins of endothelial cells, we hypothesized that these 2 genes are critical determinants of virulence. To test this hypothesis, we compared the virulence wild-type, empty plasmid–transformed, and RNAi-transformed *R. oryzae* using our DKA mouse model of *R. oryzae* pneumonia (25). Although infection in this model is initiated by intratracheal inoculation, the infection hematogenously disseminates to other target organs, such as the brain (25). Whereas empty plasmid–transformed *R. oryzae* was as virulent as wild-type *R. oryzae* (median survival time, wild-type, 3 days; empty plasmid, 4 days; $P = 0.33$), mice infected with RNAi-transformed *R. oryzae* had attenuated virulence, with a 10-day median survival time and one-third of animals surviving the lethal infection ($P = 0.003$; Figure 8A). Additionally, mice infected with RNAi-transformed *R. oryzae* had significantly lower fungal burden in the lungs and brains (primary and secondary target organs; ref. 25) than did mice infected with wild-type or empty plasmid–transformed *R. oryzae* (Figure 8B).

To confirm that the RNAi construct inhibited *CotH2* and *CotH3*, we assessed the pattern of in vivo expression of these genes in fungi recovered from the same mouse organs that were processed for tissue fungal burden. Relative to the fungal *ACT1* housekeeping gene, *CotH1* had no detectable expression in mice infected with wild-type, empty plasmid–transformed, or RNAi-transformed *R. oryzae*. In contrast, *CotH2* expression increased 4- and 2-fold in the lungs and brains, respectively, of mice infected with wild-type and empty plasmid–transformed *R. oryzae* (Figure 8C). Furthermore, *CotH3* had significantly higher expression than *CotH2* in the lungs, but not in the brains, of mice infected with wild-type or empty plasmid–transformed *R. oryzae*. Finally, fungal cells recovered from mice infected with RNAi-transformed *R. oryzae* had no expression of any of the *CotH* genes. These results indicate that *CotH2* and *CotH3* are expressed in vivo and that the reduced virulence in mice infected with RNAi-transformed *R. oryzae* is due to lack of expression of any of the *CotH* genes.

To compare infection severity, we conducted histopathological examination. Lungs harvested from mice infected with RNAi-transformed *R. oryzae* had minimal inflammation and edema and lacked any apparent presence of fungal elements. In contrast, lungs from mice infected with wild-type or empty plasmid–transformed *R. oryzae* had abundant fungal abscesses, characterized by

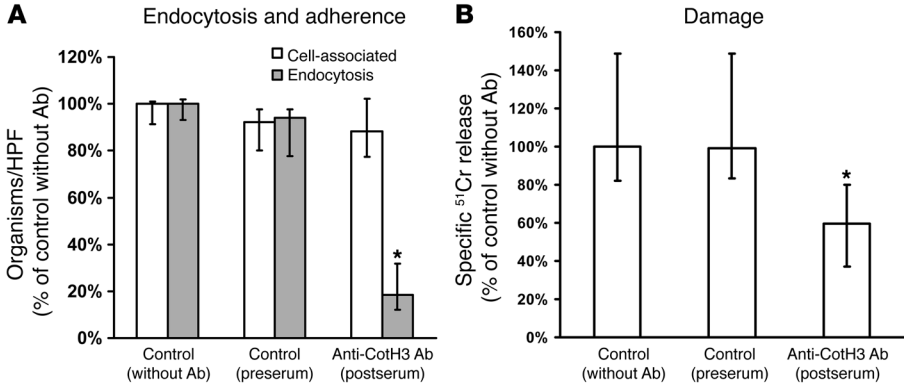

Figure 4

Anti-CotH3 Abs block endothelial cell endocytosis of and damage by *R. oryzae*. Endothelial cells were incubated with 50 μg/ml anti-CotH3, with serum from the same rabbit prior to vaccination (preserum control), for 1 hour prior to addition of *R. oryzae* germlings. (**A**) Adherence and endocytosis (determined by differential fluorescence) assays were carried out using endothelial cells split on 12-mm glass coverslips. Blocking of CotH3 and CotH2 (since the Abs react to CotH2 proteins) abrogated endocytosis of *R. oryzae* by endothelial cells. Data were derived from >700 fungal cells interacting with approximately 200 endothelial cells/group/experiment, with an average of 59% cells being endocytosed in the control. (**B**) Damage was carried out using the 96-well plate ^{51}Cr release method. Blocking of CotH3 and CotH2 reduced the ability of *R. oryzae* to cause endothelial cell damage. **P* < 0.01 vs. either control, Wilcoxon rank-sum test. *n* = 6 slides or wells per group from 3 (**A**) or 2 (**B**) independent experiments. Data are median ± interquartile range.

phagocyte infiltration and substantial edema (Figure 8D). Collectively, these data demonstrated that *CotH2* and *CotH3* are required for maximal virulence of *R. oryzae*.

Anti-CotH Abs are protective against R. oryzae infection in mice. To determine the potential for abrogation of CotH function as a treatment for mucormycosis, we treated DKA mice with the anti-CotH Abs that blocked *R. oryzae*–induced invasion of and damage to endothelial cells in vitro. Ab treatment started 2 hours before or 24 hours after intratracheal infection with *R. oryzae*. The efficacy of the anti-CotH purified IgG with >1:100,000 titer (determined by ELISA plates coated with the CotH peptide) was compared with that of preimmune IgG collected from the same rabbit prior to vaccination. DKA mice that received anti-CotH IgG prior to infection had marked improvement in survival compared with mice treated with preimmune IgG (Figure 9A). More importantly, even when the Abs were administered 24 hours after infection, 50% of mice survived (Figure 9B). These data validate our in vitro findings and support the development of potential immunotherapeutic interventions using CotH proteins as targets against mucormycosis.

Discussion

We previously determined that Mucorales, including *R. oryzae*, bind GRP78, leading to endothelial cell invasion and damage (15). A natural progression of the GRP78 work was to identify the Mucorales ligand for GRP78. Here, we provide multiple layers of evidence that the CotH family (in particular CotH3) is the fungal ligand for GRP78. First, we identified CotH proteins using far-Western blotting using GRP78 as bait, demonstrating direct interaction with CotH. Second, heterologous expression of CotH2 and CotH3 in the nonadhering/noninvasive *S. cerevisiae* resulted in the yeast binding to GRP78 in endothelial cell membrane protein extracts, and adherence to and invasion of both endothelial cells and GRP78-overexpressing CHO cells. Third, CotH colocalized with GRP78 when empty plasmid–transformed *R. oryzae* invaded endothelial cells, whereas *R. oryzae* transformed with *CotH2*/*CotH3* RNAi constructs did not. Fourth, anti-CotH Abs blocked fungal invasion and subsequent damage to endothelial cells in vitro.

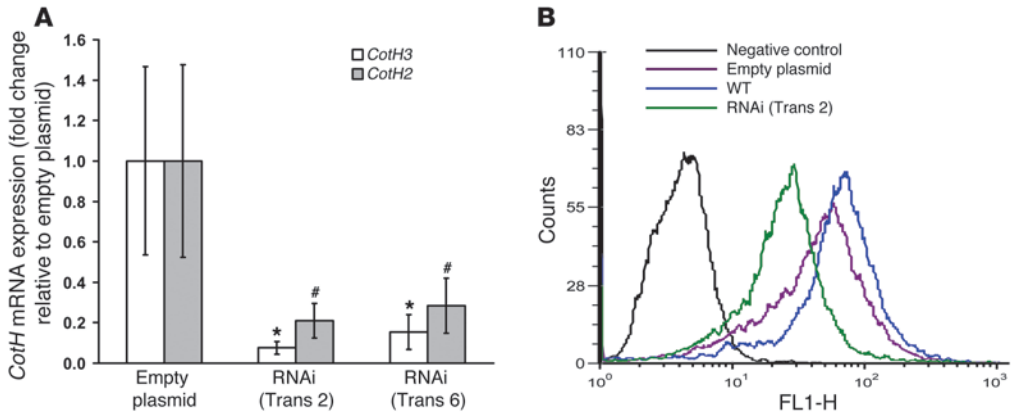

Figure 5

RNAi targeting *CotH2* and *CotH3* inhibits the expression of both genes and reduces CotH2 and CotH3 protein synthesis on the cell surface. *R. oryzae* was transformed with an RNAi construct targeting *CotH2* and *CotH3* expression or with empty plasmid. (**A**) 2 transformants demonstrated >80% reduction in *CotH2* and *CotH3* expression relative to empty plasmid–transformed *R. oryzae*, as determined by qRT-PCR. (**B**) Flow cytometry testing using anti-CotH Abs demonstrated reduced cell surface expression of CotH proteins on RNAi-transformed *R. oryzae* compared with empty plasmid–transformed, wild-type, or negative control (stained with commercial IgG instead of anti-CotH Abs) *R. oryzae*. **P* < 0.001, #*P* < 0.005 vs. empty plasmid, Wilcoxon rank-sum test. *n* = 6 per group from 2 independent experiments.

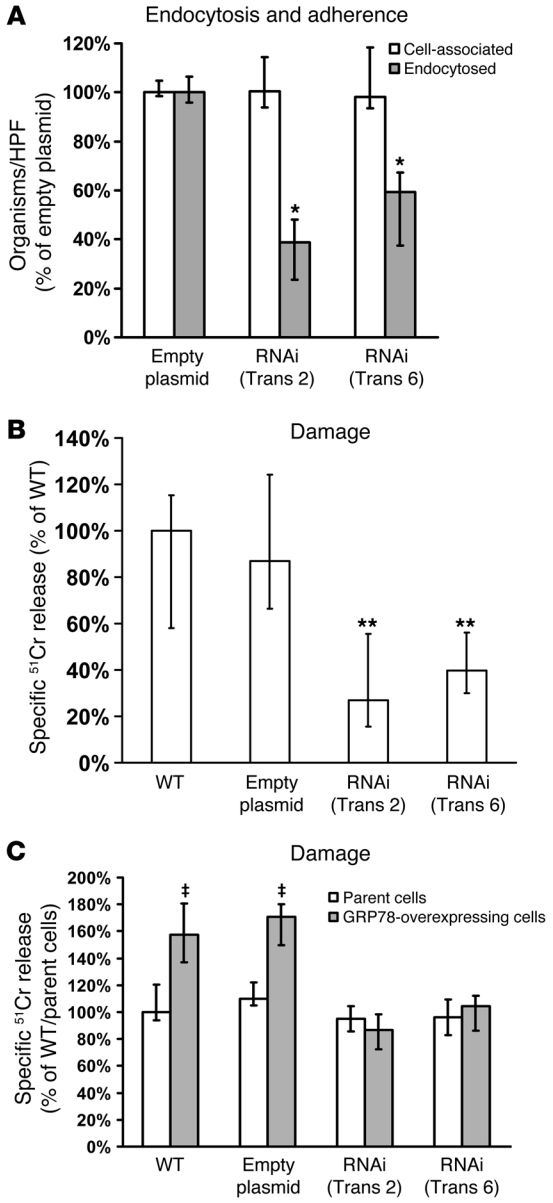

Figure 6
Inhibition of *CotH2* and *CotH3* expression decreases the ability of *R. oryzae* to invade and damage endothelial cells and GRP78-overexpressing CHO cells. (**A** and **B**) RNAi-transformed *R. oryzae* germlings caused less invasion (**A**) and damage (**B**) to endothelial cells compared with empty plasmid–transformed *R. oryzae*. (**C**) RNAi-transformed *R. oryzae* caused equivalent damage to GRP78-overexpressing versus parent CHO cells. Conversely, wild-type or empty plasmid–transformed *R. oryzae* germlings caused significantly more damage to GRP78-overexpressing cells. $^{*}P < 0.005$ vs. empty plasmid, $^{**}P < 0.01$ vs. wild-type and empty plasmid, $^{‡}P < 0.01$ vs. parent cells, Wilcoxon rank-sum test. $n = 6$ slides/group (**A**) or 9 wells/group (**B**) from 3 independent experiments. Data are median ± interquartile range.

Finally, the RNAi-transformed *R. oryzae*, with inhibition of *CotH2* and *CotH3* gene expression, had a reduced capacity to invade and damage endothelial cells and GRP78-overexpressing CHO cells.

Although heterologous expression of CotH3 and CotH2 enhanced *S. cerevisiae* adhesion to and invasion of host cells via GRP78, only invasion was abrogated when *CotH2* and *CotH3* function was interrupted in *R. oryzae*, not adherence. These results were concordant with our prior findings that adhesion and invasion of *R. oryzae* to host cells are independent processes mediated by different receptors (15). The independence of adhesion and invasion processes has been also reported for *Candida albicans* (26). The probable explanation for the adhesion function of CotH proteins when expressed in *S. cerevisiae* is that although CotH can mediate both adherence and invasion, in *R. oryzae*, other adhesins likely exist and can compensate for the loss of CotH function.

Our present results also demonstrated that CotH3 had the highest affinity to GRP78, followed by CotH2, whereas CotH1 did not bind GRP78 nor enhance *S. cerevisiae* interaction with host cells. This finding was expected, since CotH3 and CotH2 were closely related proteins with approximately 77% identity at the amino acid level, while CotH1 had only 46% identity to CotH2 or CotH3. Our homology modeling and in silico docking studies provided a predicted structural basis for the functional interactions of CotH3 and CotH2 with GRP78. Molecular modeling indicated that CotH3 conforms to a bimodal secondary structure that affords a corresponding and energetically favorable facet for binding to GRP78 (Figure 7). Importantly, this region of GRP78 encompasses the amino acid sequence used to raise Abs that inhibited endothelial cell invasion in vitro and protected mice against mucormycosis (Figures 4 and 9). Accordingly, CotH2 appears to interact with GRP78 via a smaller but substantial contact surface, consistent with our above-described biological observations. Our docking results were also consistent with the biological observation that CotH1 interacts only minimally with the GRP78 target protein.

Our in vitro data also indicated that adhesion/invasion are the primary function of the CotH proteins, since attenuation of CotH2 and CotH3 expression did not alter the susceptibility of *R. oryzae* to cell wall stressors, change the sensitivity of the mold to phagocyte-mediated damage, nor affect the cells' growth, respiration, germination, or size. However, Mucorales are not considered primary pathogens, but rather accidental ones when the host is immunocompromised. It is highly likely that CotH proteins primarily evolved to aid these fungi in being successful saprophytic organisms by facilitating adhesion to organic matter.

Our in vivo data demonstrated the importance of CotH proteins in virulence. The RNAi-transformed *R. oryzae* strain, with silenced CotH2 and CotH3, attenuated virulence in DKA mice (Figure 8). Notably, the reduced severity of inflammation and edema of lungs infected with RNAi-transformed *R. oryzae* suggests that CotH2/CotH3 may also be important for the interaction of *R. oryzae* with lung epithelial cells. However, approximately 60% of mice infected with RNAi-transformed *R. oryzae* died, which suggests the possible requirement of alternative invasins for virulence. The importance of *CotH2* and *CotH3* in *R. oryzae* virulence was further manifested in the in vivo expression of the genes relative to *CotH1*. *CotH2* and *CotH3* mRNA was expressed more highly in lungs than brains. This can be explained by the fact that, in this model, the lungs represent a primary seeded organ as a result of intratracheal inoculation, whereas brain infection happens after hematogenous dissemination occurs due to angioinvasion. The need for adhesin/invasin expression at early disease stages is likely to be higher than that after infection is established. Most interestingly, anti-CotH Abs raised against amino acids predicted to interact with GRP78

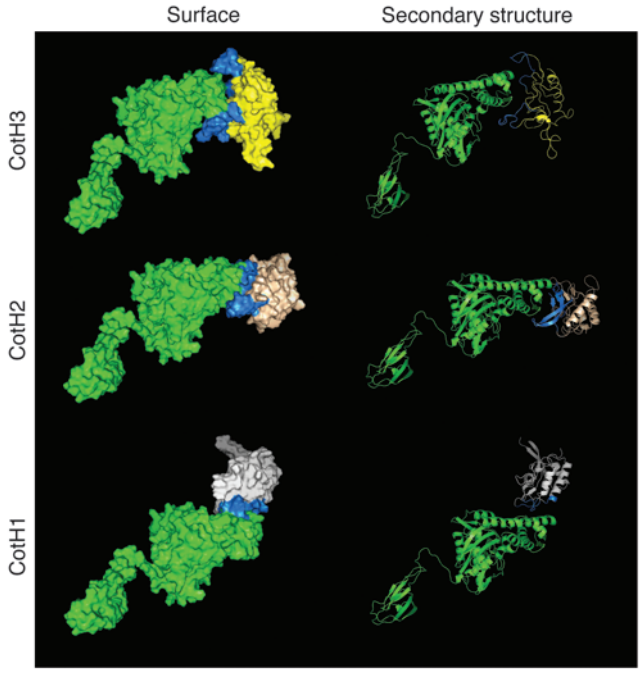

Figure 7
Comparative binding models of CotH proteins to GRP78. Models of CotH proteins were generated by homology threading from templates with known structures determined by crystallography. Molecular docking was then evaluated using CotH protein as the ligand and GRP78 as the target. The visualized water-accessible surface areas and secondary structures were energy-minimized for CotH3 (yellow), CotH2 (beige), or CotH1 (white) binding to GRP78 (green). Comparative contact areas of respective CotH proteins are shown in blue. Note the large, bimodal binding cleft in CotH3 that was also partially present in CotH2, consistent with biological findings. In contrast, CotH1 exhibited a limited contact area on a distinct aspect of the GRP78 target protein. Of interest are the comparative structural domains that may confer GRP78 interactions by differing CotH proteins. For example, each of the CotH proteins has multiple α-helical domains that appear to serve as a structural scaffold. However, the proteins differ considerably in the extent of their β-sheet conformation. For example, CotH3 exhibits an extended docking-predicted GRP78 contact facet, with little β-sheet stabilization. Conversely, CotH2 and, to a lesser extent, CotH1 contain explicit β-sheet structural domains. In the former case, this domain forms a component of the GRP78-docking facet. In the latter, the β-sheet domain does not appear to be involved in interactions with GRP78. Thus, despite similarities in their overall topology, more specific 3D aspects likely determine the capability for distinct CotH protein interactions with GRP78.

protected DKA mice from *R. oryzae* infection. Collectively, these results demonstrated that CotH proteins are required for *R. oryzae* virulence and strongly indicate their promise as targets for development of therapeutic interventions against mucormycosis.

CotH proteins are the third identified invasins among fungal human pathogens. The *C. albicans* Als3 protein was reported to mediate invasion of human umbilical vein endothelial cells and epithelial cells via binding to N-cadherin and E-cadherin, respectively (27). Additionally, Als3 protein facilitates invasion of *C. albicans* to brain microvascular endothelial cells via binding to the heat shock protein Gp96 (28). The cell surface protein Ssa1 also mediates *C. albicans* invasion of brain microvascular endothelial cells, via binding to a receptor that is yet to be identified (28). To our knowledge, the CotH family represents the first identified invasins in human pathogenic molds. It is interesting that despite the lack of structural homology between the CotH and Als3 families, they both bind heat shock proteins (albeit different ones) of a mammalian host. This emphasizes the diversity of fungal invasins that use similar targets to invade host cells.

We previously found that elevated iron and glucose concentrations, which are frequently seen in DKA patients, enhance GRP78 expression on the host cell surface, increasing invasion and damage of endothelial cells (15). These data serve to explain why patients with elevated serum iron and glucose concentrations are uniquely susceptible to mucormycosis. In the present study, the CotH family of proteins was found to be highly conserved among Mucorales organisms that are known to cause invasive disease (Table 1). CotH proteins were present in *Mucor* spp., *Lichtheimia*, *Rhizomucor*, *Mortierella*, and *Lentamyces*, which are known to cause invasive infections to mammals and to other Mucorales (29–35). Notably, the CotH family was not present in any other organisms, including *Conidiobolus coronatus*, which was previously classified as a Zygomycete and causes superficial infections (2). These findings serve to additionally explain why patients with elevated serum iron and glucose (e.g., DKA, other forms of acidosis, and hyperglycemia) are uniquely susceptible to mucormycosis. Not only is GRP78 overexpressed in these conditions, but also the ligand that binds to the receptor is only present in Mucorales known to cause invasive disease. Furthermore, the uniqueness of CotH proteins to Mucorales and their in vivo expression during mucormycosis makes this protein family a prime target for developing diagnostic tools critically needed for early detection of mucormycosis (36, 37). Investigation of *CotH* genes and their proteins in early detection of mucormycosis infections is currently ongoing.

In summary, we have identified the fungal ligand that binds to GRP78 host receptor during mucormycosis. CotH3 and, to a lesser extent, CotH2 were responsible for attaching *R. oryzae* to cell surface GRP78 during invasion of host cells. These proteins were required for full virulence of *R. oryzae*, and anti-CotH Abs protected DKA mice from mucormycosis. Additionally, the CotH family of proteins was universally conserved in Mucorales and absent from other pathogens. Collectively, these findings further explain the unique susceptibility of patients with hyperglycemia, DKA, and other forms of acidosis to mucormycosis. Finally, our data strongly suggest that the *CotH* family of genes and their products are prime targets for the development of immunotherapeutic and diagnostics strategies against mucormycosis.

Methods

Organisms and culture conditions. Several clinical Mucorales isolates were used in this study. *R. oryzae* 99-880 and *Mucor* sp. 99-932 are brain isolates, whereas *R. oryzae* 99-892 and *Rhizopus* sp. 99-1150 were isolated from lungs of infected patients and obtained from the Fungus Testing Laboratory of University of Texas Health Science Center at San Antonio. *C. bertholletiae* 182, also a clinical isolate, was a gift from T. Walsh (Weill Cornell Medical College of Cornell University, New York, New York, USA). *L. corymbifera* is also a clinical isolate obtained from the DEFEAT Mucor clinical study (38). All wild-type Mucorales were grown on potato dextrose agar (PDA; BD Diagnostic) plates, whereas *R. oryzae* M16 (a *pyrF*-null mutant unable to synthesize its own uracil that has been previously characterized in full;

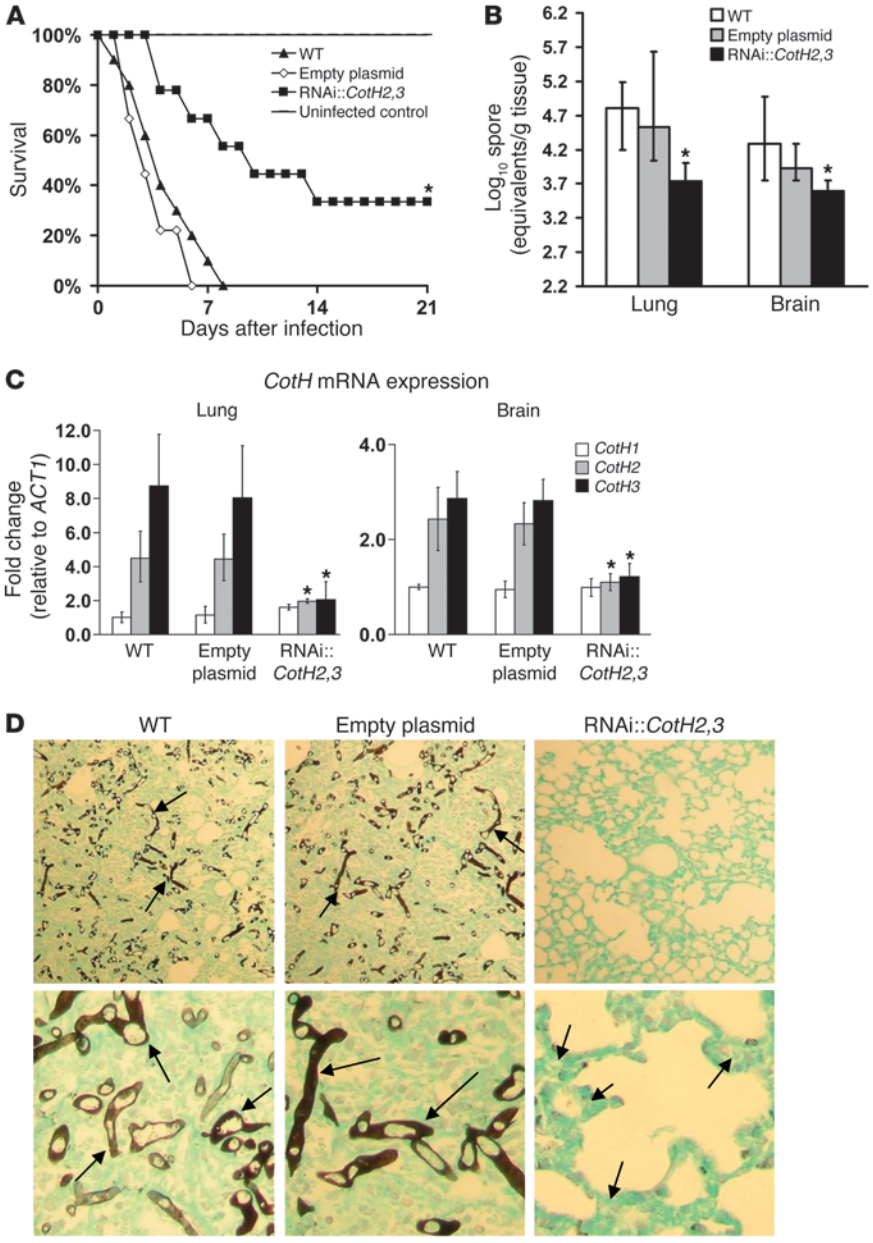

Figure 8

Inhibition of *CotH2* and *CotH3* expression attenuates *R. oryzae* virulence in DKA mice. (**A**) Survival of mice infected intratracheally with wild-type (n = 10), empty plasmid–transformed (n = 9), and RNAi-transformed (n = 9) *R. oryzae* (inhaled inocula, 2.4 × 10^3, 2.8 × 10^3, and 2.5 × 10^3 spores, respectively). *P < 0.003 vs. wild-type and empty plasmid, log-rank test. (**B**) Lungs and brain fungal burden of DKA mice (n = 9 per group) infected intratracheally with wild-type, empty plasmid–transformed, or RNAi-transformed cells (1.7 × 10^3, 3.0 × 10^3, and 3.1 × 10^3, respectively). Mice were sacrificed on day +2 relative to infection, and their organs were processed for tissue fungal burden, determined by qPCR. Data are median ± interquartile range. *P < 0.001 versus wild-type and empty plasmid, Wilcoxon rank-sum test. (**C**) In vivo expression of *CotH* genes in lungs and brains harvested from mice infected with wild-type, empty plasmid–transformed, or RNAi-transformed *R. oryzae*, as determined by qRT-PCR using specific primers to each *CotH* gene. Data are mean ± SD. *P < 0.001 vs. wild-type and empty plasmid. (**D**) PAS-stained sections of lungs demonstrated extensive hyphal elements (arrows) and signs of severe pneumonia from organs collected from DKA mice infected with wild-type or empty plasmid–transformed *R. oryzae*, whereas mild pneumonia (arrows) was observed in lungs from mice infected with RNAi-transformed *R. oryzae*. Original magnification, ×100 (top); ×400 (bottom).

ref. 39) was grown on PDA supplemented with 100 μg/ml uracil. Mucorales were grown for 5–7 days at 37°C. Sporangiospores were collected in endotoxin-free Dulbecco PBS containing 0.01% Tween 80, washed with PBS, and counted with a hemocytometer to prepare the final inocula. To form germlings, spores were incubated in liquid yeast extract–peptone–dextrose (YPD; 1% yeast extract [Difco Laboratories], 2% bacto-peptone [Difco], 2% glucose [Sigma-Aldrich]) medium at 37°C with shaking for 1–3 hours based on the assay. Germlings were washed twice with RPMI 1640 without glutamine (Irvine Scientific) for all assays used, except for the GRP78 affinity experiments, in which germlings were washed twice with PBS containing Ca^{2+} and Mg^{2+} (PBS-CM).

S. cerevisiae strain ATCC 62956 (LL-20), which is *his3*Δ and *leu2*Δ, was constructed by L. Lau (University of Illinois at Chicago, Chicago, Illinois, USA) (40) and acted as the host for CotH expression plasmids (see below). This strain was maintained on YPD supplemented with 60 μg/ml L-leucine and 2 μg/ml L-histidine. To induce expression of *CotH* genes, transformants were grown on yeast nitrogen base (YNB; Difco) medium supplemented with 0.5% ammonium sulfate, 2% galactose (Difco). To suppress the expression of *CotH* genes, 2% D-glucose was substituted for galactose. *S. cerevisiae* blastospores were collected in PBS after growing the organisms in the medium under investigation at 30°C overnight. Yeast cells were counted using a hemocytometer to prepare the final inocula. In all media above, 2% agar (Difco) was used to solidify the medium.

Protoplast formation and collection of R. oryzae cell wall material. To identify the *R. oryzae* ligand that binds to endothelial cell GRP78, we collected cell wall material from supernatants of protoplasts of *R. oryzae* germlings. Briefly, *R. oryzae* spores (6 × 10^6) were germinated in YPD medium for 3 hours at 37°C. Germinated cells were collected by centrifugation at 900 *g*, washed twice with 0.5M sorbitol, and then resuspended in 0.5 M sorbitol in sodium phosphate buffer (pH 6.4). Protoplasting solution con-

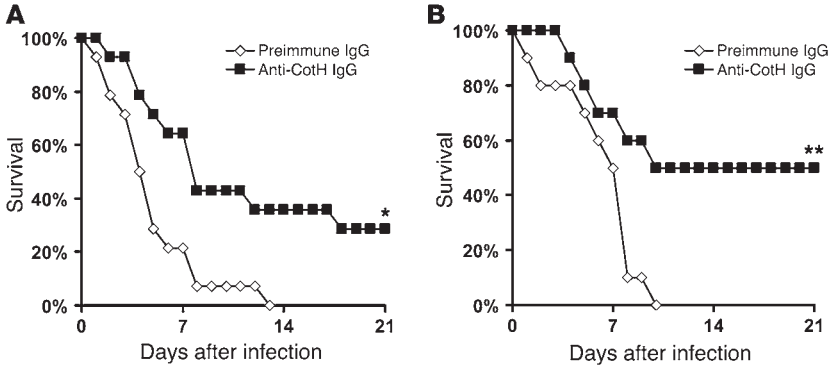

Figure 9
Anti-CotH Abs protect DKA mice from *R. oryzae* infection. DKA mice were treated with 1 mg purified IgG collected from rabbit serum after vaccination with CotH3 peptide. Abs were administered intraperitoneally to mice either 2 hours before (**A**) or 24 hours after (**B**) infecting them intratracheally with 2.5×10^5 wild-type *R. oryzae* spores. Average delivered inoculum to the lungs was 6.0×10^3 (**A**) and 3.8×10^3 (**B**) spores. $n = 14$ (**A**), 10 (**B**) per arm. $^*P = 0.005$, $^{**}P = 0.02$, log-rank test.

sisting of 310 mg/ml lysing enzymes (Sigma-Aldrich), 30 mg/ml chitnase (Sigma-Aldrich), and 10 mg/ml chitosinase (US Biological) was added to the germinated spores and incubated with gentle shaking at 30°C for 2 hours. Protoplasts were collected by centrifugation for 5 minutes at 200 *g* at 4°C, washed twice with 0.5 M sorbitol, and resuspended in the same buffer. Incubating protoplasts in the presence of the osmotic stabilizer sorbitol enables regeneration of the cell wall, and during regeneration, cell wall constituents are released into the supernatant (41, 42). After a 2-hour incubation period (43), protoplasts were pelleted, and the supernatant was sterilized by filtration (0.22-μm filters) in the presence of protease inhibitors (Pierce). The supernatant was concentrated, and protein concentration was measured using the Bradford method (BioRad). Negative control samples were processed similarly, with the exception of the absence of protoplasts.

Heterologous expression of CotH genes in S. cerevisiae. Total RNA was isolated from *R. oryzae* spores grown on PDA plate and reverse transcribed into cDNA. The entire ORF of *CotH1*, *CotH2*, and *CotH3* (see http://www.broadinstitute.org/annotation/genome/rhizopus_oryzae/MultiHome.html for sequences) were PCR amplified from cDNA using Phusion high-fidelity PCR Kit (New England Biolabs) and the primers listed in Table 2. The amplified PCR fragments were cloned into pESC-LEU yeast dual expression vector (Stratagene) in the *BamHI* and *SalI* sites downstream of the *Gal1* promoter, so that expression of the putative ligands could be induced by galactose-containing medium. Cloning of each of the amplified fragments was carried out using In-Fusion 2.0 Dry-Down PCR Cloning Kit (Clontech Laboratories), per the manufacturer's instructions. The generated yeast expression vectors were independently transformed into *S. cerevisiae* strain LL-20 by the polyethylene glycol-lithium acetate method, and transformants were screened on the YNB medium lacking leucine. *S. cerevisiae* LL-20 transformed with the empty plasmid served as a control.

Cell surface localization and expression of CotH proteins. We raised rabbit polyclonal Abs against a peptide from CotH3 predicted to be highly antigenic and cell surface expressed. Peptide MGQTNDGAYRDPTDNN (which has 78% identity to CotH1 and CotH2) was coupled with KLH and used to commercially vaccinate rabbits (ProMab Biotechnologies Inc.). Purified IgG from the vaccinated rabbits was used to detect cell surface localization of CotH proteins on *S. cerevisiae* and on *R. oryzae* interacting with endothelial cells. To determine the cell surface expression of each CotH protein on the transformed *S. cerevisiae*, blastospores (10^5 cells/ml) from galactose-containing medium were incubated with the anti-CotH IgG at 1:100 for 1 hour on ice after a blocking step using 1.5% goat serum in PBS for 1 hour. Cells were washed 3 times with Tris-buffered saline (TBS; 0.01 M Tris HCl [pH 7.4], 0.15 M NaCl) containing 0.05% Tween 20, then counterstained with FITC-labeled goat anti-rabbit IgG at 1:100 for 1 hour on ice. The stained cells were imaged with Leica confocal microscope using an excitation wavelength of 488 nm.

To quantify the expression of CotH proteins on *R. oryzae* cell surface, spores were germinated in YPD for 3 hours at 37°C. Germlings were stained with the anti-CotH IgG as above, then 1-ml samples were analyzed using a FACSCalibur (Becton Dickinson) instrument equipped with an argon laser emitting at 488 nm. Fluorescence emission was read with a 515/40 bandpass filter. Fluorescence data were collected with logarithmic amplifiers. The mean fluorescence intensities of 10^4 events were calculated using CELLQUEST software (44, 45).

Endothelial cells and CHO cells. Endothelial cells were collected from umbilical vein endothelial cells by the method of Jaffe et al. (46). Cells were harvested using collagenase and grown in M-199 (Gibco, Invitrogen) enriched with 10% FBS, 10% defined bovine calf serum, L-glutamine, penicillin, and streptomycin (all from Gemini Bio-Products). Second-passage cells were grown to confluence in 24- or 96-well tissue culture plates (Costar) on fibronectin (BD Biosciences). All incubations were in 5% CO_2 at 37°C. Reagents were tested for endotoxin using a chromogenic limulus amebocyte lysate assay (BioWhittaker Inc.), and endotoxin concentrations were <0.01 IU/ml. The CHO cell line C.1, derived from parental DHFR-deficient CHO cells engineered to overexpress GRP78, were a gift of A. Lee (University of Southern California Keck School of Medicine, Los Angeles, California, USA; refs. 20, 21).

Extraction of endothelial cell membrane proteins. Endothelial cell membrane proteins were extracted according to the method of Isberg and Leong (19). Briefly, confluent endothelial cells in 100-mm-diameter tissue culture dishes were rinsed twice with warm PBS-CM and then incubated with Ez-Link Sulfo-NHS-LS Biotin (0.5 mg/ml; Pierce) in PBS-CM for 12 minutes at 37°C in 5% CO_2. Cells were then rinsed extensively with cold PBS-CM and scraped from the tissue culture dishes. Endothelial cells were collected by centrifugation at 500 *g* for 5 minutes at 4°C, then lysed by incubation for 20 minutes on ice in PBS-CM containing 5.8% *n*-octyl-β-D-glucopyranoside (w/v) (Cal BioChem) and protease inhibitors (1 mM phenylmethyl sulfonyl fluoride, 1 μg/ml pepstatin A, 1 μg/ml leupeptin, and 1 μg/ml aprotinin; Sigma-Aldrich). Cell debris was removed by centrifugation at 5,000 *g* for 5 minutes at 4°C. The supernatant was collected and centrifuged at 100,000 *g* for 1 hour at 4°C. The concentration of the endothelial cell proteins in the resulting supernatant was determined using the Bradford method (BioRad).

Binding of endothelial cell GRP78 by CotH-expressing S. cerevisiae. 8×10^8 *S. cerevisiae* cells expressing *CotH1*, *CotH2*, *CotH3*, or empty plasmid were incubated for 1 hour on ice with 250 μg biotin-labeled endothelial cell surface proteins in PBS-CM plus 1.5% *n*-octyl-β-D-glucopyranoside and protease inhibitors. Unbound endothelial cell proteins were washed away by 3 rinses with this buffer. The endothelial cell proteins that remained bound to the fungal cells were eluted twice with 6M urea (Fluka), and the supernatant was combined and concentrated to appropriate volume with a Microcon centrifugal filter (10,000 MWCO; Millipore). Proteins were then separated on 10% SDS-PAGE and transferred to PVDF-plus membranes

Table 2
Oligonucleotides used in this study

Primer name	Primer sequence	Description
Clone into pESC-Leu expression plasmid and detect gene expression via RT-PCR		
CotH1 forward	AAAAAACCCCGGATCCTATGAAATCCCTACTTTTTGTTGTATTC	5′ primer (amplifying 1,830 bp)
CotH1 reverse	TCTGTTCCATGTCGACCTAGAAGAAAGAGGCAAATAAAGTGC	3′ primer (amplifying 1,830 bp)
CotH2 forward	AAAAACCCCGGATCCTATGAAATTATCACTCACTATAGTATCCTCT	5′ primer (amplifying 1,785 bp)
CotH2 reverse	TCTGTTCCATGTCGACTTAAAAGATAGCAGTGGCAACTAAAG	3′ primer (amplifying 1,785 bp)
CotH3 forward	AAAAAACCCCGGATCCTATGAAATTATCTATTATATCCGCTGCC	5′ primer (amplifying 1,806 bp)
CotH3 reverse	TCTGTTCCATGTCGACTTAGAATACAAGGAGAGCTAAAGCG	3′ primer (amplifying 1,806 bp)
Detect gene expression of the fourth putative ligand via RT-PCR		
RO3G_16295	AAAAAACCCCGGATCCTATGATTGCTACCCCTTTTGAAA	5′ primer (amplifying 1,098 bp)
RO3G_16295	TCTGTTCCATGTCGACTTAAAAGAAAATAAAGAATGTTGCAGC	3′ primer (amplifying 1,098 bp)
Detect CotH3 in other Mucorales		
CotH3 forward ORF	ATGAAATTATCTATTATATCCGCTGCC	5′ primer (amplifying 1913 bp)
CotH3 reverse ORF	TTAGAATACAAGGAGAGCTAAAGCG	3′ primer (amplifying 1913 bp)
Construct RNAi plasmid		
RNAi-cotH3 forward	GCATGCTAGAACAGAAGAAAGTTTTGATCGTTC	5′ primer (amplifying 450 bp)
RNAi-cotH3 reverse	GTACGACGTTCACGAATCTGTGTAGG	3′ primer (amplifying 450 bp)
RNAi-cotH3I forward	CCGCGGGACGTTCACGAATCTGTGTAGG	5′ inverted primer (amplifying 450 bp)
RNAi-cotH3I reverse	GCTAGCAGAACAGAAGAAAGTTTTGATCGTTC	3′ inverted primer (amplifying 450 bp)
Quantitatively detect *CotH* gene expression in vitro and in vivo		
CotH1 forward	CAAACAAATGATGGGGCCTA	5′ primer (amplifying 104 bp)
CotH1 reverse	CGTTTTTGTTCAAGATTTACACCA	3′ primer (amplifying 104 bp)
CotH2 forward	CCTAATAAGGACAACGCAAACG	5′ primer (amplifying 101 bp)
CotH2 reverse	TTGGCAATGGCTGTGTTATC	3′ primer (amplifying 101 bp)
CotH3 forward	GCCAATCCTAATGGTGAAGC	5′ primer (amplifying 126 bp)
CotH3 reverse	CATGAAACGGTCGAGATCAA	3′ primer (amplifying 126 bp)
Actin forward	AGCTCCTTTGAACCCCAAGT	5′ primer (amplifying 121 bp)
Actin reverse	ACGACCAGAGGCATACAAGG	3′ primer (amplifying 121 bp)
Determine tissue fungal burden via qPCR		
RO 18sRNA forward	GCGGATCGCATGGCC	5′ primer (amplifying 57 bp)
RO 18sRNA reverse	CCATGATAGGGCAGAAAATCG	3′ primer (amplifying 57 bp)

(GE Water & Process Technologies). The membrane was then treated with Western Blocking Reagent (Roche) and probed with a rabbit anti-GRP78 Ab (Abcam) followed with secondary Abs of HRP-conjugated goat anti-rabbit IgG (Pierce). After incubation with SuperSignal West Dura Extended Duration Substrate (Pierce), signals were detected using a CCD camera.

Colocalization of GRP78 with CotH protein on phagocytosed R. oryzae germlings by indirect immunofluorescence. We used a modification of our previously described method (15, 26). Confluent endothelial cells on a 12-mm-diameter glass coverslip were infected with 10^5/ml RPMI 1640 medium *R. oryzae* cells that had pregerminated for 1 hour. After a 60-minute incubation at 37°C, cells were gently washed twice with HBSS to remove unbound organisms, then fixed with 3% paraformaldehyde. After washing with 1% BSA (Fisher) prepared in PBS-CM, cells were incubated for 1 hour with 1:100 mouse monoclonal anti-GRP78 Ab (BD Biosciences). Coverslips were washed in 1% BSA in PBS, then counterstained with 1:100 Alexa Fluor 488–labeled goat anti-mouse IgG (Invitrogen). Cells were then permeabilized for 5 minutes in 0.5% Triton X-100 and incubated with 1:100 rabbit anti-CotH polyclonal Ab for 1 hour, followed by Alexa Fluor 568–labeled goat anti-rabbit IgG (Molecular Probes) for 1 hour. After washing, the coverslip was mounted on a glass slide with a drop of ProLong Gold antifade reagent (Molecular Probes) and viewed by confocal microscopy. The final confocal images were produced by combining optical sections taken through *z* axis.

Interaction of fungi with endothelial or CHO cells. The number of organisms endocytosed by endothelial cells or CHO cells was determined using a modification of our previously described differential fluorescence assay (47). Briefly, 12-mm glass coverslips in a 24-well cell culture plate were coated with fibronectin for at least 4 hours and seeded with endothelial or CHO cells until confluence. After washing twice with prewarmed HBSS (Irvine Scientific), cells were then infected with 10^5 cells of *S. cerevisiae* expressing *CotH* or *R. oryzae* in RPMI 1640 medium that had germinated for 1 hour. After incubation for 3 hours, cells were fixed in 3% paraformaldehyde and stained for 1 hour with 1% Uvitex (gift from J. Isharani, Ciba-Geigy, Greensboro, North Carolina, USA), which specifically binds to the chitin of the fungal cell wall. After washing 3 times with PBS, coverslips were mounted on a glass slide with a drop of ProLong Gold antifade reagent (Molecular Probes) and sealed with nail polish. The total number of cell-associated organisms (i.e., germlings adhering to monolayer) was determined by phase-contrast microscopy. The same field was examined by epifluorescence microscopy, and the number of uninternalized germlings (which were brightly fluorescent) was determined. The number of endocytosed organisms was calculated by subtracting the number of fluorescent organisms from the total number of visible organisms. At least 400 organisms were counted in 20–40 different fields per slide. 2 slides per arm were used for each experiment, and the experiment was performed in triplicate on different days.

R. oryzae–induced endothelial or CHO cell damage was quantified using a ^{51}Cr release assay (48). Briefly, endothelial cells or CHO cells grown in 96-well tissue culture plates containing detachable wells were incubated with 1 μCi/well $Na_2{}^{51}CrO_4$ (ICN) in M-199 medium (for endothelial cells) or α-MEM (for CHO cells) for 16 hours. On the day of the experiment, the unincorporated ^{51}Cr was aspirated, and wells were washed twice with prewarmed HBSS. Cells were infected with fungal germlings (1.5×10^5 germinated for 1 hour) suspended in 150 μl RPMI 1640 medium supplemented with glutamine. Spontaneous ^{51}Cr release was determined by incubating endothelial or CHO cells in RPMI 1640 medium supplemented with glutamine without *R. oryzae*. After 3 hours of incubation at 37°C in a 5% CO_2 incubator, 50% of the medium was aspirated from each well and transferred to glass tubes, and cells were manually detached and placed into another set of tubes. The amount of ^{51}Cr in the aspirate and the detached well was determined by gamma counting. The total amount of ^{51}Cr incorporated by endothelial cells in each well was calculated as the sum of radioactive counts per minute of the aspirated medium and radioactive counts of the corresponding detached wells. After data were corrected for variations in the amount of tracer incorporated in each well, the percentage of specific endothelial cell release of ^{51}Cr was calculated as follows: [(experimental release × 2) – (spontaneous release × 2)]/[total incorporation – (spontaneous release × 2)]. Each experimental condition was tested at least in triplicate, and the experiment was repeated at least once.

For Ab blocking of adherence, endocytosis, or damage caused by *R. oryzae*, assays were carried out as above, except that endothelial cells were incubated with 50 μg anti-CotH IgG (raised against CotH3 peptides predicted to be antigenic), or with serum obtained from the same rabbit prior to vaccination, for 1 hour prior to adding *R. oryzae* germlings.

RNAi of CotH2/CotH3. We used our previously described RNAi technology (24) to inhibit the expression of *CotH2* and *CotH3* in *R. oryzae*. A 450-bp fragment commonly shared between *CotH2* and *CotH3* ORF (Table 2) was PCR amplified and cloned as an inverted repeat under control of the *Rhizopus* expression vector pRNAi-pdc-intron (49). The generated plasmid was transformed into the *R. oryzae pyrF* mutant (strain M16) using the biolistic delivery system (BioRad), and transformants were selected on minimal medium lacking uracil (50).

Cell surface expression of CotH proteins on *R. oryzae* germlings was quantified using FACS analysis. Briefly, *R. oryzae* germlings grown in YNB without uracil for 4 hours were blocked with 10% goat serum, then stained with anti-CotH polyclonal Abs raised against a 16-mer peptide (MGQTNDGAYRDPTDNN) from CotH3 in rabbits (primary Ab) at 1:100 for 1 hour. Germlings were counterstained with Alexa Fluor 488–labeled anti-rabbit IgG at 1:100 for 1 hour. *R. oryzae* germlings stained with preimmune serum collected from the same rabbit were used as negative control. A FACSCalibur (BD) instrument equipped with an argon laser emitting at 488 nm was used for flow cytometric analysis. Fluorescence data were collected with logarithmic amplifiers. The population percent fluorescence of 5×10^3 events was calculated using CELLQUEST software.

The growth rate of wild-type, empty plasmid–transformed, or RNAi-transformed *R. oryzae* was quantified by plating 10^5 spores in 10 μl on YPD or minimal medium without uracil, and plates were incubated at 37°C for 16 hours, after which colony diameter was measured. The effect of *CotH2/CotH3* silencing on *R. oryzae* germination was also determined by germinating 5×10^4/ml wild-type, empty plasmid–transformed, or RNAi-transformed *R. oryzae* in YPD for 2, 3, 4, and 5 hours. At specific time points, a sample from each culture was visualized under a light microscope, and germ tube length was recorded for 100 cells using a micrometer. Finally, the effect of *CotH2/CotH3* inhibition on *R. oryzae* respiratory activity was assessed using XTT-menadione assay (51). Briefly, 10^4 spores/ml of wild-type, empty plasmid–transformed, or RNAi-transformed *R. oryzae* were incubated in RPMI 1640 with glutamine (Cambrex Bio Science Inc.) buffered with 0.165 M 3-*N*-morpholinopropanesulfonic acid (MOPS; pH 7.0) at 37°C in 96-well plate for 6 hours. 50 μl XTT-menadione solution (containing 200 μg/ml XTT and 25 μM menadione; both from Sigma-Aldrich) was added to the 96-well plates to allow for conversion of XTT to its formazan derivative. The plate was shaken for 1–2 minutes at 100 rpm until complete dissolution of the formazan derivatives, then incubated at 37°C for an additional 2 hours. XTT conversion was measured using DYNEX MRX Revelation microtiter plate reader (BioSurplus) at an OD of 450 nm. XTT conversion by metabolically active cells was calculated after subtracting the background OD of simultaneously incubated wells containing media and reagents without spores.

The effect of *CotH2/CotH3* inhibition on *R. oryzae* susceptibility to mouse neutrophils and the mouse macrophage cell lines RAW and J774 was determined by comparing the damage of empty plasmid– or RNAi-transformed *R. oryzae* (51). Briefly, the XTT-menadione assay was used as above, except that *R. oryzae* (10^4 spores/ml) was incubated with the macrophage cell lines at 2×10^5/ml (1:20 target/effector ratio) or with neutrophils at 10^5/ml (1:10 target/effector ratio).

To determine the effect of the anti-CotH Abs on growth rate, germination, and respiration of wild-type *R. oryzae*, the assays used above were carried out in the presence of 10 μg/ml pre- or postimmune IgG.

Effect of CotH2 and CotH3 downregulation on the cell wall integrity of R. oryzae. Because *CotH2* and *CotH3* encode cell wall proteins, we sought to investigate the effect of downregulation of these 2 genes on cell wall integrity. 5 μl of different spore numbers of wild-type, empty plasmid–transformed, or RNAi-transformed *R. oryzae* were plated on YNB with or without cell wall stressors of hydrogen peroxide, Congo red 2 mg/ml, SDS (0.004%), calcofluor (0.1 mg/ml), and Tition X100 (0.1%). The plates were incubated at 37°C for 16 hours before measuring the colony diameter.

Computational modeling and protein docking. Refined models of CotH1, CotH2, and CotH3 proteins were generated by conjugate gradient energy minimization (HyperChem, version 8.0.2, CHARMM 27 parameter set; ref. 52) and models of the full-length proteins used for in silico docking studies. An X-ray structure of human GRP78 (MMDB ID 88213) was used as appropriate for validation (53). Preliminary docking of the proteins was done with ZDock (version 3.0.2; http://zlab.umassmed.edu/zdock/; ref. 54). Comparative docking of each CotH protein to the GRP78 protein target was performed with RosettaDock (version 3.2; ref. 55) using the ROSIE server (http://rosettadock.graylab.jhu.edu/docking; ref. 56). In brief, the docking method used rigid-body Monte Carlo searches and optimization of backbone displacement and side-chain conformations using Monte Carlo minimization. The initial docking search rendered approximately 1,000 decoys for each ligand. Interaction sites were ranked by binding energy and by the energy contribution per residue (3Å radius). Ligand-protein residue pairs were then ranked based on total energy contribution and orientation-dependent hydrogen bonding. Iterative refinement yielded 10 best scoring structures predicted for each ligand, and the lowest-energy ranked ensemble was used as a final docked model.

In vivo virulence studies and passive immunization. Male ICR mice (≥20 g) were all purchased from Taconic and housed in groups of 5 each. They were given irradiated feed and sterile water containing 50 μg/ml Baytril (Bayer) ad libitum. Mice were rendered DKA with a single i.p. injection of 190 mg/kg streptozotocin in 0.2 ml citrate buffer 10 days prior to fungal challenge (57). Glycosuria and ketonuria were confirmed in all mice 7 days after streptozotocin treatment. Additionally, on days –2 and +3 relative to infection, mice were given a dose of cortisone acetate (250 mg/kg s.c.). DKA mice were infected intratracheally with fungal spores after sedation with ketamine (66 mg/kg; Phoenix) and xylazine (4.8 mg/kg; Lloyd Laboratories), with a target inoculum of 2.5×10^5 spores in 25 μl. To confirm the inoculum,

3 mice were sacrificed immediately after inoculation, their lungs were homogenized in PBS and quantitatively cultured on PDA plates containing 0.1% triton, and colonies were counted after a 24-hour incubation period at 37°C. The primary efficacy endpoint was time to moribundity. In some experiments, as a secondary endpoint, fungal burden in the lungs and brains (primary and secondary target organs) was determined 48 hours after infection by quantitative PCR assay, as we previously described (58). Values were expressed as $\log_{10}$ spore equivalent/g tissue. Histopathological examination was carried out on sections of the harvested organs after fixing in 10% zinc formalin. The fixed organs were embedded in paraffin, and 5-mm sections were stained with H&E or PAS to detect *R. oryzae* hyphae (45).

For in vivo expression of *CotH* genes, lungs and brains collected from mice 48 hours after wild-type, empty plasmid–transformed, or RNAi-transformed *R. oryzae* infection were flash frozen in liquid nitrogen and processed for RNA extraction using a Tri Reagent solution (Ambion). Reverse transcription was performed with RETROscript (Ambion) using primers listed in Table 2. For quantitative RT-PCR, SYBR green assays were performed. Constitutively expressed *ACT1* was used as a control for all reactions. Calculations and statistical analyses were performed using StepOne Real-Time PCR System (Applied Biosystems).

To investigate whether anti-CotH polyclonal Abs raised against the 16-mer peptide (MGQTNDGAYRDPTDNN) protected mice from *R. oryzae* infection, we administered 1 mg IgG purified from rabbit sera collected before (control) or after immunization with the peptide (test) to DKA mice. IgG was injected intraperitoneally 2 hours before or 24 hours after intratracheal infection of DKA mice with 2.5×10^5 spores in 25 μl PBS (25). Mouse survival was monitored for 21 days after infection, and any moribund mice were euthanized. Results were plotted using Kaplan-Meier survival curves.

Statistics. Differences in *CotH* expression and fungi–endothelial cell interactions were compared by nonparametric Wilcoxon rank-sum test. The nonparametric log-rank test was used to determine differences in survival times. A P value less than 0.05 was considered significant.

Study approval. All procedures involving mice were approved by the IACUC of the Los Angeles Biomedical Research Institute at Harbor-UCLA Medical Center, according to the NIH guidelines for animal housing and care. Human endothelial cell collection was approved by the IRB of the Los Angeles Biomedical Research Institute at Harbor-UCLA Medical Center. Because umbilical cords are collected without donor identifiers, the IRB considers them medical waste not subject to informed consent.

Acknowledgments

This work was supported by Public Health Service grants R01 AI063503 and R21 AI082414-01 to A.S. Ibrahim. Collection of human umbilical cord endothelial cells was supported by the National Center for Advancing Translational Sciences through UCLA CTSI grant UL1TR000124. S.G. Filler is supported by grant R01 AI054928. The genome sequencing of Mucorales strains for this project has been funded in part with federal funds from the National Institute of Allergy and Infectious Diseases, NIH, Department of Health and Human Services (contract no. HHSN272200900009C). The authors acknowledge the technical assistance of Samuel French for reading the histopathological slides, Yue Fu for helping in the design of the heterologous expression of *CotH* genes, Qi Su for assembling the Mucorales genome sequenced by University of Maryland and performing the nucleotide blast, and the perinatal nurses of the Harbor-UCLA General Clinical Research Center for collecting umbilical cords. We also thank Kerstin Voigt for making the CotH sequence of *L. corymbifera* and *Lentamyces parricida* available to us, and Shawn Lockhart for providing some of the DNA samples for the genome sequencing project. Finally, we thank Thomas Walsh for providing us with the *C. bertholletiae* clinical isolate. The research described herein was conducted in part at the research facilities of the Los Angeles Biomedical Research Institute at Harbor-UCLA Medical Center.

Received for publication May 31, 2013, and accepted in revised form October 3, 2013.

Address correspondence to: Ashraf S. Ibrahim, Los Angeles Biomedical Research Institute, Division of Infectious Diseases, Harbor-UCLA Medical Center, 1124 West Carson St., St. John's Cardiovascular Research Center, Torrance, California 90502, USA. Phone: 310.222.6424; Fax: 310.782.2016; E-mail: ibrahim@labiomed.org.

This work was presented at the 51st Interscience Conference on Antimicrobial Agents and Chemotherapy in Chicago, Illinois, USA, on September 17–20, 2011 (abstract no. M-398), and at the 18th Congress of the International Society for Human and Animal Mycology in Berlin, Germany, on June 11–15, 2012 (abstract no. WG15-3).

1. Sugar A. Agents of mucormycosis and related species. In: Mandell GL, Bennett JE, Dolin R, eds. *Principles and Practice of Infectious Diseases*. Philadelphia, Pennsylvania, USA: Elsevier; 2005:2979.
2. Ibrahim AS, Edwards JJE, Filler SG, Spellberg B. Mucormycosis and entomophthoramycosis (zygomycosis). In: Kauffman CA, Pappas PG, Sobel JD, Dismukes WE, eds. *Essentials of Clinical Mycology*. New York, New York, USA: Springer; 2011:265–280.
3. Ribes J, Vanover-Sams CL, Baker DJ. Zygomycetes in human disease. *Clin Microbiol Rev*. 2000; 13(2):236–301.
4. Ibrahim A. Host cell invasion in mucormycosis: role of iron. *Curr Opin Microbiol*. 2011;14(4):406–411.
5. Spellberg B, Walsh TJ, Kontoyiannis DP, Edwards J Jr, Ibrahim AS. Recent advances in the management of mucormycosis: from bench to bedside. *Clin Infect Dis*. 2009;48(12):1743–1751.
6. Kauffman CA. Zygomycosis: reemergence of an old pathogen. *Clin Infect Dis*. 2004;39(4):588–590.
7. Roden M, et al. Epidemiology and outcome of zygomycosis: a review of 929 reported cases. *Clin Infect Dis*. 2005;41(5):634–653.
8. Ibrahim AS, Spellberg B, Walsh TJ, Kontoyiannis DP. Pathogenesis of mucormycosis. *Clin Infect Dis*. 2012;54(suppl 1):S16–S22.
9. Spellberg B, Edwards J Jr, Ibrahim A. Novel perspectives on mucormycosis: pathophysiology, presentation, and management. *Clin Microbiol Rev*. 2005;18(3):556–569.
10. Neblett Fanfair R, et al. Necrotizing cutaneous mucormycosis after a tornado in Joplin, Missouri, in 2011. *N Engl J Med*. 2012;367(23):2214–2225.
11. Petrikkos G, Skiada A, Lortholary O, Roilides E, Walsh TJ, Kontoyiannis DP. Epidemiology and clinical manifestations of mucormycosis. *Clin Infect Dis*. 2012;54(suppl 1):S23–S34.
12. Artis W, Fountain JA, Delcher HK, Jones HE. A mechanism of susceptibility to mucormycosis in diabetic ketoacidosis: transferrin and iron availability. *Diabetes*. 1982;31(12):1109–1114.
13. Ibrahim A, Edwards JEJ, Filler SG. Zygomycosis. In: Dismukes WE, Pappas PG, Sobel JD, eds. *Clinical Mycology*. New York, New York, USA: Oxford University Press; 2003:241–251.
14. Ibrahim A, Spellberg B, Avanessian V, Fu Y, Edwards JE Jr. Rhizopus oryzae adheres to, is phagocytosed by, and damages endothelial cells in vitro. *Infect Immun*. 2005;73(2):778–783.
15. Liu M, et al. The endothelial cell receptor GRP78 is required for mucormycosis pathogenesis in diabetic mice. *J Clin Invest*. 2010;120(6):1914–1924.
16. Wu Y, Li Q, Chen XZ. Detecting protein-protein interactions by Far western blotting. *Nat Protoc*. 2007;2(12):3278–3284.
17. Naclerio G, Baccigalupi L, Zilhao R, De Felice M, Ricca E. Erratum. Bacillus subtilis spore coat assembly requires cotH gene expression. *J Bacteriol*. 1996;178(21):6407.
18. Giorno R, et al. Morphogenesis of the Bacillus anthracis spore. *J Bacteriol*. 2007;189(3):691–705.
19. Isberg RR, Leong JM. Multiple beta 1 chain integrins are receptors for invasin, a protein that promotes bacterial penetration into mammalian cells. *Cell*. 1990;60(5):861–871.
20. Morris J, Dorner AJ, Edwards CA, Hendershot LM, Kaufman RJ. Immunoglobulin binding protein (BiP) function is required to protect cells from endoplasmic reticulum stress but is not required for the secretion of selective proteins. *J Biol Chem*. 1997; 272(7):4327–4334.
21. Reddy R, Mao C, Baumeister P, Austin RC, Kaufman RJ, Lee AS. Endoplasmic reticulum chaperone protein GRP78 protects cells from apoptosis induced by topoisomerase inhibitors: role of ATP binding site in suppression of caspase-7 activation. *J Biol Chem*. 2003;278(23):20915–20924.
22. Li J, Lee AS. Stress induction of GRP78/BiP and its

role in cancer. *Curr Mol Med*. 2006;6(1):45–54.
23. Davidson D, et al. Kringle 5 of human plasminogen induces apoptosis of endothelial and tumor cells through surface-expressed glucose-regulated protein 78. *Cancer Res*. 2005;65(11):4663–4672.
24. Ibrahim A, et al. The high affinity iron permease is a key virulence factor required for Rhizopus oryzae pathogenesis. *Mol Microbiol*. 2010;77(3):587–604.
25. Luo G, et al. Efficacy of liposomal amphotericin B and posaconazole in intratracheal models of murine mucormycosis. *Antimicrob Agents Chemother*. 2013;57(7):3340–3347.
26. Phan Q, Fratti RA, Prasadarao NV, Edwards JE Jr, Filler SG. N-cadherin mediates endocytosis of Candida albicans by endothelial cells. *J Biol Chem*. 2005;280(11):10455–10461.
27. Phan Q, et al. Als3 is a Candida albicans invasin that binds to cadherins and induces endocytosis by host cells. *PLoS Biol*. 2007;5(3):e64.
28. Liu Y, Mittal R, Solis NV, Prasadarao NV, Filler SG. Mechanisms of Candida albicans trafficking to the brain. *PLoS Pathog*. 2011;7(10):e1002305.
29. Nosari A, et al. Mucormycosis in hematologic malignancies: an emerging fungal infection. *Haematologica*. 2000;85(10):1068–1071.
30. Eickhardt S, et al. A non-fatal case of invasive zygomycete (Lichtheimia corymbifera) infection in an allogeneic haematopoietic cell transplant recipient. *APMIS*. 2012;121(5):456–459.
31. Skiada A, et al. Zygomycosis in Europe: analysis of 230 cases accrued by the registry of the European Confederation of Medical Mycology (ECMM) Working Group on Zygomycosis between 2005 and 2007. *Clin Microbiol Infect*. 2011;17(12):1859–1867.
32. Gomes M, Lewis RE, Kontoyiannis DP. Mucormycosis caused by unusual mucormycetes, non-Rhizopus, -Mucor, and -Lichtheimia species. *Clin Microbiol Rev*. 2011;24(2):411–445.
33. MacDonald S, Corbel MJ. Mortierella wolfii infection in cattle in Britain. *Vet Rec*. 1981;109(19):419–421.
34. Uzal F, Connole MD, O'Boyle D, Dobrenov B, Kelly WR. Mortierella wolfii isolated from the liver of a cow in Australia. *Vet Rec*. 1999;145(9):260–261.
35. Hoffmann K, Voigt K. Absidia parricida plays a dominant role in biotrophic fusion parasitism among mucoralean fungi (Zygomycetes): Lentamyces, a new genus for A. parricida and A. zychae. *Plant Biol (Stuttg)*. 2009;11(4):537–554.
36. Walsh TJ, Gamaletsou MN, McGinnis MR, Hayden RT, Kontoyiannis DP. Early clinical and laboratory diagnosis of invasive pulmonary, extrapulmonary, and disseminated mucormycosis (zygomycosis). *Clin Infect Dis*. 2012;54(suppl 1):S55–S60.
37. Walsh T, Chanock SJ. Diagnosis of invasive fungal infections: advances in nonculture systems. *Curr Clin Top Infect Dis*. 1998;18:101–153.
38. Spellberg B, et al. The Deferasirox-AmBisome Therapy for Mucormycosis (DEFEAT Mucor) study: a randomized, double-blinded, placebo-controlled trial. *J Antimicrob Chemother*. 2012;67(3):715–722.
39. Skory C, Ibrahim AS. Native and modified lactate dehydrogenase expression in a fumaric acid producing isolate Rhizopus oryzae 99–880. *Curr Genet*. 2007;52(1):23–33.
40. Orr-Weaver T, Szostak JW, Rothstein RJ. Yeast transformation: a model system for the study of recombination. *Proc Natl Acad Sci U S A*. 1981; 78(10):6354–6358.
41. Pitarch A, Jimenez A, Nombela C, Gil C. Decoding serological response to Candida cell wall immunome into novel diagnostic, prognostic, and therapeutic candidates for systemic candidiasis by proteomic and bioinformatic analyses. *Mol Cell Proteomics*. 2006;5(1):79–96.
42. Pitarch A, et al. Two-dimensional gel electrophoresis as analytical tool for identifying Candida albicans immunogenic proteins. *Electrophoresis*. 1999; 20(4–5):1001–1010.
43. Michielse C, et al. Development of a system for integrative and stable transformation of the zygomycete Rhizopus oryzae by Agrobacterium-mediated DNA transfer. *Mol Genet Genomics*. 2004;271(4):499–510.
44. Fu Y, et al. Candida albicans Als1p: an adhesin that is a downstream effector of the EFG1 filamentation pathway. *Mol Microbiol*. 2002;44(1):61–72.
45. Ibrahim A, et al. The iron chelator deferasirox protects mice from mucormycosis through iron starvation. *J Clin Invest*. 2007;117(9):2649–2657.
46. Jaffe E, Nachman RL, Becker CG, Minick CR. Culture of human endothelial cells derived from umbilical veins. Identification by morphologic and immunologic criteria. *J Clin Invest*. 1973;52(11):2745–2756.
47. Ibrahim A, Filler SG, Alcouloumre MS, Kozel TR, Edwards JE Jr, Ghannoum MA. Adherence to and damage of endothelial cells by Cryptococcus neoformans in vitro: role of the capsule. *Infect Immun*. 1995;63(11):4368–4374.
48. Ibrahim A, et al. Bacterial endosymbiosis is widely present among zygomycetes but does not contribute to the pathogenesis of mucormycosis. *J Infect Dis*. 2008;198(7):1083–1090.
49. Mertens J, Skory CD, Ibrahim AS. Plasmids for expression of heterologous proteins in Rhizopus oryzae. *Arch Microbiol*. 2006;186(1):41–50.
50. Skory C. Homologous recombination and double-strand break repair in the transformation of Rhizopus oryzae. *Mol Genet Genomics*. 2002;268(3):397–406.
51. Antachopoulos C, Meletiadis J, Roilides E, Sein T, Walsh TJ. Rapid susceptibility testing of medically important zygomycetes by XTT assay. *J Clin Microbiol*. 2006;44(2):553–560.
52. Polak E, Ribiere G. Note sur la xonvergence de directions conjugees. *Rev Francaise Informat Recherche Operatinelle*. 1969;16:35–43.
53. Macias A, et al. Adenosine-derived inhibitors of 78 kDa glucose regulated protein (Grp78) ATPase: insights into isoform selectivity. *J Med Chem*. 2011; 54(12):4034–4041.
54. Chen R, Li L, Weng Z. ZDOCK: an initial-stage protein-docking algorithm. *Proteins*. 2003;52(1):80–87.
55. Chaudhury S, Berrondo M, Weitzner BD, Muthu P, Bergman H, Gray JJ. Benchmarking and analysis of protein docking performance in Rosetta v3.2. *PLoS One*. 2011;6(8):e22477.
56. Lyskov S, Gray JJ. The RosettaDock server for local protein-protein docking. *Nucleic Acids Res*. 2008;36(Web Server issue):W233–W238.
57. Ibrahim A, Avanessian V, Spellberg B, Edwards JE Jr. Liposomal amphotericin B, and not amphotericin B deoxycholate, improves survival of diabetic mice infected with Rhizopus oryzae. *Antimicrob Agents Chemother*. 2003;47(10):3343–3344.
58. Ibrahim A, et al. Caspofungin inhibits Rhizopus oryzae 1,3-beta-D-glucan synthase, lowers burden in brain measured by quantitative PCR, and improves survival at a low but not a high dose during murine disseminated zygomycosis. *Antimicrob Agents Chemother*. 2005;49(2):721–727.